Inorg. Chem. **2007**, *46*, 2181–2186

Syntheses, Structures, and Magnetic Properties of the Face-Centered Cubic Clusters $[Tp_8(H_2O)_{12}M_6Fe_8(CN)_{24}]^{4+}$ (M = Co, Ni)

Long Jiang,[†] Hye Jin Choi,[‡] Xiao-Long Feng,[†] Tong-Bu Lu,*[,†] and Jeffrey R. Long*[,‡]

MOE Key Laboratory of Bioinorganic and Synthetic Chemistry, State Key Laboratory of Optoelectronic Materials and Technologies, and Instrumentation Analysis & Research Center, Sun Yat-Sen University, Guangzhou 510275, China, and the Department of Chemistry, University of California, Berkeley, California 94720

Received October 9, 2006

Reactions between $K[TpFe(CN)_3]$ (Tp^- = hydrotris(1-pyrazolyl)borate) and $M(ClO_4)_2 \cdot 6H_2O$ (M = Co or Ni) in a mixture of acetonitrile and methanol afford, upon crystallization via THF vapor diffusion, $[Tp_8(H_2O)_{12}Co_6Fe_8(CN)_{24}](ClO_4)_4 \cdot 12THF \cdot 7H_2O$ (**1**) and $[Tp_8(H_2O)_{12}Ni_6Fe_8(CN)_{24}](ClO_4)_4 \cdot 12THF \cdot 7H_2O$ (**2**). Both compounds contain cyano-bridged clusters with a face-centered cubic geometry, wherein octahedral Co^{II} or Ni^{II} centers are situated at the face-centering sites. The results of variable-temperature magnetic susceptibility measurements indicate the presence of ferromagnetic exchange coupling within both molecules to give ground states of $S = 7$ and 10, respectively. Low-temperature magnetization data reveal significant zero-field splitting, with the best fits for the Co_6Fe_8 and Ni_6Fe_8 clusters yielding $D = -0.54$ and 0.21 cm^{-1}, respectively; ac magnetic susceptibility measurements performed on both samples showed no evidence of the slow relaxation effects associated with single-molecule magnet behavior.

Introduction

Recently, there has been a surge of interest in single-molecule magnets, molecular clusters exhibiting slow magnetic relaxation by the combined effect of a high spin ground state, S, and a negative uniaxial magnetic anisotropy, D.[1] Loss of degeneracy of the ground-state M_S levels in such molecules creates an energy barrier for spin reversal from $M_S = +S$ to $M_S = -S$, given by $U = S^2|D|$ for integer S values or $U = (S^2 - {}^1/_4)|D|$ for half-integer S values. Thus, below the blocking temperature, the magnetization of an individual molecule can be trapped in either a spin-up or spin-down orientation, producing a bistability that is attractive for a variety of potential applications.[2] Since discovery of the first single-molecule magnet, $[Mn_{12}O_{12}(MeCO_2)_{16}(H_2O)_4]$, with $U \approx 50$ cm^{-1},[1] numerous other molecules have been demonstrated to exhibit similar behavior, with most early work focusing on metal−oxo-type clusters.[3]

As an alternative strategy for the synthesis of new single-molecule magnets, cyanometalate complexes have also been employed in the assembly of high-spin cluster compounds.[4] Here, the simplicity of the coordination chemistry enables a ligand-directed approach to cluster synthesis, as well as some substitutional control over the ensuing magnetic properties.

* To whom correspondence should be addressed. E-mail: lutongbu@mail.sysu.edu.cn (T.B.L.); jrlong@berkeley.edu (J.R.L.).

† Sun Yat-Sen University.

‡ University of California, Berkeley.

(1) (a) Sessoli, R.; Tsai, H. L.; Schake, A. R.; Wang, S.; Vincent, J. B.; Folting, K.; Gatteschi, D.; Christou, G.; Hendrickson, D. N. *J. Am. Chem. Soc.* **1993**, *115*, 1804. (b) Sessoli, R.; Gatteschi, D.; Caneschi, A.; Novak, M. A. *Nature* **1993**, *365*, 141.

(2) (a) Garanin, D. A.; Chudnovsky, E. M. *Phys. Rev. B* **1997**, *56*, 11102. (b) Leuenberger, M. N.; Loss, D. *Nature* **2001**, *410*, 789. (c) Tejada, J. *Polyhedron* **2001**, *20*, 1751. (d) Jo, M.-H.; Grose, J. E.; Baheti, K.; Deshmukh, M. M.; Sokol, J. J.; Rumberger, E. M.; Hendrickson, D. N.; Long, J. R.; Park, H.; Ralph, D. C. *Nano Lett.* **2006**, *6*, 2014.

(3) (a) Barrar, A. L.; Debrunner, P.; Gatteschi, D.; Schulz, C. E.; Sessoli, R. *Europhys. Lett.* **1996**, *35*, 133. (b) Castro, S. L.; Sun, Z.; Grant, C. M.; Bollinger, J. C.; Hendrickson, D. N.; Christou, G. *J. Am. Chem. Soc.* **1998**, *120*, 2365. (c) Barrar, A. L.; Caneschi, A.; Cornia, A. Fabrizi, B. F.; Gatteschi, D.; Sangregorio, C.; Sessoli, R. Sorace, L. *J. Am. Chem. Soc.* **1999**, *121*, 5302. (d) Boskovic, C.; Pink, M.; Huffman, J. C.; Hendrickson, D. N.; Christou, G. *J. Am. Chem. Soc.* **2001**, *123*, 9914. (e) Boskovic, C.; Brechin, E. K.; Streib, W. E.; Folting, K.; Bollinger, J. C.; Hendrickson, D. N.; Christou, G. *J. Am. Chem. Soc.* **2002**, *124*, 3725. (f) Tasiopoulos, A. J.; Wernsdorfer, W.; Moulton, B.; Zaworotko, M. J.; Christou, G. *J. Am. Chem. Soc.* **2003**, *125*, 15274. (g) Oshio, H.; Hoshino, N.; Ito, T.; Nakano, M. *J. Am. Chem. Soc.* **2004**, *126*, 8805. (h) Coronado, E.; Forment-Aliaga, A.; Gaita-Ariño, A.; Giménez-Saiz, C.; Romero, F. M.; Wernsdorfer, W. *Angew. Chem., Int. Ed.* **2004**, *43*, 6152. (i) Rajaraman, G.; Murugesu, M.; Sañudo, E. C.; Soler, M.; Wernsdorfer, W.; Helliwell, M.; Muryn, C.; Raftery, J.; Teat, S. J.; Christou, G.; Brechin, E. K. *J. Am. Chem. Soc.* **2004**, *126*, 15445. (j) Maheswaran, S.; Chastanet, G.; Teat, S. J.; Mallah, T.; Sessoli, R.; Wernsdorfer, W.; Winpenny, R. E. P. *Angew. Chem., Int. Ed.* **2005**, *44*, 5044.

10.1021/ic061924b CCC: $37.00
Published on Web 01/26/2007

For example, the use of 1,4,7-triazacyclononane (tacn) as a blocking ligand permits formation of cyano-bridged cubic clusters, such as $[(tacn)_8Co_8(CN)_{12}]^{12+}$, in accordance with the reaction[5]

$$4[(tacn)M(H_2O)_3]^{x+} + 4[(tacn)M'(CN)_3]^{y-} \rightarrow [(tacn)_8M_4M'_4(CN)_{12}]^{4(x-y)+} \quad (1)$$

The application of a similar approach and various capping ligands has generated a series of related cubic clusters, certain members of which possess the magnetic anisotropy required in a single-molecule magnet: $Ni^{II}_4Fe^{III}_4$,[6] $Co^{II}_4Co^{III}_4$,[6a] $Ni^{II}_4Co^{III}_4$,[6a] $Rh^{III}_4Co^{III}_4$,[7] $Co^{III}_4Ru^{II}_4$,[8] $Mo^0_4Rh^{IV}_4$,[9] $Mn^{II}_4Re^{II}_4$,[10] $Fe^{III}_4Re^{I}_4$,[11] and $Co^{II}_4Re^{II}_4$.[11] Thus far, however, the highest-spin ground state achieved for such a simple cubic geometry is $S = 6$.[6]

To increase the spin of the ground state and thereby, potentially, the spin-reversal barrier U, methods for synthesizing larger metal-cyanide clusters are under development. Along this line of investigation, reactions analogous to reaction 1 with a tridentate blocking ligand on only one of the reactants were found to generate a 14-metal cluster[12]

$$6[Ni(H_2O)_6]^{2+} + 8[(Me_3tacn)Cr(CN)_3] \rightarrow [(Me_3tacn)_8Cr_8Ni_6(CN)_{24}]^{12+} \quad (2)$$

The structure of the product features a cube of eight Cr^{III} centers connected through cyanide bridges to six Ni^{II} centers, one situated just above the center of each cube face. Because of the thermally assisted isomerization of the cyanide ligands in the course of the reaction, the Ni^{II} centers are low-spin ($S = 0$) with a square planar coordination geometry. The performance of the reaction at lower temperatures led to a metastable compound containing high-spin Ni^{II} ($S = 1$), which displayed magnetic properties consistent with an $S = 18$ ground state, but unfortunately, it could not be crystallized. It was hypothesized that this metastable species was a face-centered cubic cluster, "$[(Me_3tacn)_8(H_2O)_{12}Ni_6Cr_8(CN)_{24}]^{12+}$", in which the cyanide bridges had not yet reoriented and the additional water ligands gave rise to octahedral coordination at the six face-centering Ni^{II} sites. While several other face-centered cubic clusters have since been crystallized,[6a,13] only one contains paramagnetic metal centers at both the corner and the face-centering sites: $[Tp_8(H_2O)_6Cu_6Fe_8(CN)_{24}]^{4+}$ ($Tp^- =$ hydrotris(1-pyrazolyl)-borate).[14] Here, the face-centering Cu^{II} ions exhibit square pyramidal coordination, and ferromagnetic coupling with the low-spin Fe^{III} ions gives rise to an $S = 7$ ground state. Although ac magnetic susceptibility measurements suggested single-molecule magnet behavior for this cluster, its spin reversal barrier was too small to measure at the accessible temperatures and switching frequencies. The replacement of the Cu^{II} ions with other higher-spin transition metals could potentially lead to single-molecule magnets with enhanced blocking temperatures but would likely require a means of incorporating octahedral metal centers.

Herein, we demonstrate such species for the first time with the synthesis of two new face-centered cubic clusters: $[Tp_8(H_2O)_{12}Co_6Fe_8(CN)_{24}]^{4+}$ and $[Tp_8(H_2O)_{12}Ni_6Fe_8(CN)_{24}]^{4+}$.

Experimental Section

Preparation of Compounds. The compound $K[TpFe(CN)_3]$ was prepared as previously reported.[15] Anhydrous methanol and acetonitrile were distilled over magnesium powder or CaH_2 under N_2. All other chemicals were used as purchased without further purification.

Caution: *Perchlorate salts of metal complexes with organic ligands are potentially explosive. They should be handled with extreme care and prepared only in small quantities.*

$[Tp_8(H_2O)_{12}Co_6Fe_8(CN)_{24}](ClO_4)_4\cdot 12THF\cdot 7H_2O$ (1). A solution of $Co(ClO_4)_2\cdot 6H_2O$ (73 mg, 0.20 mmol) in 10 mL of methanol was added to a suspension of $K[TpFe(CN)_3]$ (93 mg, 0.27 mmol) in 10 mL of acetonitrile. The mixture was stirred at room temperature for 2 h and then filtered. Diffusion of THF vapor into the filtrate afforded 110 mg (70%) of product as dark red cube-shaped crystals suitable for X-ray analysis. IR (KBr): ν_{BH} 2517, ν_{CN} 2160, 2058 cm^{-1}. Anal. Calcd. for $C_{144}H_{216}B_8Cl_4Co_6Fe_8N_{72}O_{48}$: C, 36.39; H, 4.58; N, 21.22. Found: C, 36.45; H, 4.47; N, 20.71. Molar ratio of metal ions via ICP-AA analysis: Co/Fe = 5.0:8.0.

$[Tp_8(H_2O)_{12}Ni_6Fe_8(CN)_{24}](ClO_4)_4\cdot 12THF\cdot 7H_2O$ (2). The use of $Ni(ClO_4)_2\cdot 6H_2O$ in a procedure directly analogous to that detailed

(4) (a) Mallah, T.; Auberger, C.; Verdaguer, M.; Veillet, P. *J. Chem. Soc., Chem. Commun.* **1995**, 61. (b) Sculiller, A.; Mallah, T.; Verdaguer, M.; Nivorzkhin, A.; Tholence, J.-L.; Veillet, P. *New J. Chem.* **1996**, *20*, 1. (c) Van Langenberg, K.; Batten, S. R.; Berry, K. J.; Hockless, D. C. R.; Moubaraki, B.; Murray, K. S. *Inorg. Chem.* **1997**, *36*, 5006. (d) Zhong, Z. J.; Seino, H.; Mizobe, Y.; Hidai, M.; Fujishima, A.; Ohkoshi, S.; Hashimoto, K. *J. Am. Chem. Soc.* **2000**, *122*, 2952. (f) Larionova, J.; Gross, M.; Pilkington, M.; Andres, H.; Stoeckli-Evans, H.; Güdel, H.-U.; Decurtins, S. *Angew. Chem., Int. Ed.* **2000**, *39*, 1605. (g) Sokol, J. J.; Hee, A. G.; Long, J. R. *J. Am. Chem. Soc.* **2002**, *124*, 7656. (h) Berlinguette, C. P.; Vaughn, D.; Canada-Vilalta, C.; Galan-Mascaros, J. R.; Dunbar, K. R. *Angew. Chem., Int. Ed.* **2003**, *42*, 1523. (i) Beltran, L. M. C.; Long, J. R. *Acc. Chem. Res.* **2005**, *38*, 325 and references therein. (j) Ferbinteanu, M.; Miyasaka, H.; Wernsdorf, W.; Nakata, K.; Suguira, K.; Yamashita, M.; Coulon, C.; Clérac, R. *J. Am. Chem. Soc.* **2005**, *127*, 3090. (k) Song, Y.; Zhang, P.; Ren, X.-M.; Shen, X.-F.; Li, Y.-Z.; You, X.-Z. *J. Am. Chem. Soc.* **2005**, *127*, 3708. (l) Miyasaka, H.; Takahashi, H.; Madanbashi, T.; Sugiura, K.; Clérac, R.; Nojiri, H. *Inorg. Chem.* **2005**, *44*, 5969. (m) Wang, C.-F.; Zuo, J.-L.; Bartlett, B. M.; Song, Y.; Long, J. R.; You, X.-Z. *J. Am. Chem. Soc.* **2006**, *128*, 7162. (n) Glaser, T.; Heidemeier, M.; Weyhermüller, T.; Hoffmann, R.-D.; Rupp, H.; Müller, P. *Angew. Chem., Int. Ed.* **2006**, *45*, 6033.

(5) Heinrich, J. L.; Berseth, P. A.; Long, J. R. *Chem. Commun.* **1998**, 1231.

(6) (a) Yang, J. Y.; Shores, M. P.; Sokol, J. J.; Long, J. R. *Inorg. Chem.* **2003**, *42*, 1403. (b) Li, D.; Parkin, S.; Wang, G.; Yee, G. T.; Clérac, R.; Wernsdorfer, W.; Holmes, S. M. *J. Am. Chem. Soc.* **2006**, *128*, 4214. (c) Li, D.; Parkin, S.; Clérac, R.; Holmes, S. M. *Inorg. Chem.* **2006**, *45*, 7569.

(7) (a) Klausmeyer, K. K.; Rauchfuss, T. B.; Wilson, S. R. *Angew. Chem., Int. Ed. Engl.* **1998**, *37*, 1694.

(8) Ramesh, M.; Rauchfuss, T. B. *J. Organomet. Chem.* **2004**, *689*, 1425.

(9) Klausmeyer, K. K.; Wilson, S. R.; Rauchfuss, T. B. *J. Am. Chem. Soc.* **1999**, *121*, 2705.

(10) Schelter, E. J.; Prosvirin, A. V.; Dunbar, K. R. *J. Am. Chem. Soc.* **2004**, *126*, 15004.

(11) Schelter, E. J.; Prosvirin, A. V.; Reiff, W. M.; Dunbar, K. R. *Angew. Chem., Int. Ed.* **2004**, *43*, 4912.

(12) Berseth, P. A.; Sokol, J. J.; Shores, M. P.; Heinrich, J. L.; Long, J. R. *J. Am. Chem. Soc.* **2000**, *122*, 9655.

(13) Shores, M. P.; Sokol, J. J.; Long, J. R. *J. Am. Chem. Soc.* **2002**, *122*, 2279.

(14) Wang, S.; Zuo, J. L.; Zhou, H. C.; Choi, H. J.; Ke, Y. X.; Long, J. R.; You, X. Z. *Angew. Chem., Int. Ed.* **2004**, *43*, 5940.

(15) Lescouëzec, R.; Vaissermann, J.; Lloret, F.; Julve, M.; Verdaguer, M. *Inorg. Chem.* **2002**, *41*, 5943.

Table 1. Crystallographic Data and Refinement Parameters for **1** and **2**

	1	**2**
formula	$Fe_8Co_6B_8C_{144}H_{214}N_{72}Cl_4O_{47}$	$Fe_8Ni_6B_8C_{144}H_{214}N_{72}Cl_4O_{47}$
fw	4734.53	4733.21
cryst size	0.42 × 0.37 × 0.31 mm	0.31 × 0.27 × 0.26 mm
cryst syst	cubic	cubic
space group	$Pm\bar{3}m$	$Pm\bar{3}m$
a	17.5455(3) Å	17.5480(12) Å
b	17.5455(3) Å	17.5480(12) Å
c	17.5455(3) Å	17.5480(12) Å
vol	5401.3(2) Å^3	5403.6(6) Å^3
Z	1	1
D_c	1.456 g cm^{-3}	1.455 g cm^{-3}
μ	1.101 g cm^{-3}	1.163 g cm^{-3}
reflns collected	5811	17 379
unique reflns	831 (R_{int} = 0.042)	737 (R_{int} = 0.057)
params	104	93
GOF on F^2	1.053	1.092
R1,[a] wR2[b] ($I > 2\sigma(I)$)	0.0803, 0.2073	0.0970, 0.2352
R1,[a] wR2[b] (all data)	0.1045, 0.2431	0.1097, 0.2498

[a] $R1 = \sum||F_o| - |F_c||/\sum|F_o|$. [b] $wR2 = [\sum[w(F_o^2 - F_c^2)^2]/\sum w(F_o^2)^2]^{1/2}$. Weighting: **1**, $w = 1/[\sigma^2(F_o)^2 + (0.1064P)^2 + 59.6659P]$; **2**, $w = 1/[\sigma^2(F_o)^2 + (0.1633P)^2 + 10.0951P]$, where $P = [(F_o^2) + 2F_c^2]/3$.

for the preparation of **1** afforded 96 mg (60%) of dark red cube-shaped crystals suitable for X-ray analysis. IR (KBr): ν_{BH} 2510, ν_{CN} 2169, 2126 cm^{-1}. Anal. Calcd. for $C_{144}H_{202}B_8Cl_4Fe_8N_{72}Ni_6O_{41}$: C, 37.40; H, 4.40; N, 21.81. Found: C, 37.39; H, 4.81; N, 22.10. Molar ratio of metal ions via ICP-AA analysis: Ni/Fe = 6.3:8.0.

X-ray Structure Determinations. X-ray diffraction data for single crystals of **1** and **2** were collected at 293(2) K on a Bruker Smart 1000 CCD diffractometer with Mo Kα radiation (λ = 0.71073 Å). Empirical absorption corrections were applied using the program SADABS.[16] The structures were solved using direct methods, which yielded the positions of all non-hydrogen atoms. These were refined first isotropically and then anisotropically. All hydrogen atoms of the ligands were placed in calculated positions with fixed isotropic thermal parameters and included in structure factor calculations in the final stage of full-matrix least-squares refinement. The hydrogen atoms of the water molecules were located from the difference Fourier map and refined isotropically. Disorder in the Tp^- ligands, ClO_4^- anions, and THF molecules stemming from the high symmetry of the structure (space group $Pm\bar{3}m$) was modeled using partially occupied atom positions, and the model gave a relative large *R* values. All calculations were performed using the SHELXTL software suite.[17] Crystallographic data and refinement parameters are summarized in Table 1.

Other Physical Methods. Elemental analyses were performed using an Elementar Vario EL elemental analyzer. The metal content of each sample was determined by inductively coupled plasma atomic absorption (ICP-AA) analyses using a Perkin-Elmer Optima 3000DV instrument. Infrared spectra were recorded in the 400−4000 cm^{-1} region using a Bruker EQUINOX 55 spectrophotometer.

(16) Sheldrick, G. M. *SADABS, Program for empirical absorption correction of area detector data*; University of Göttingen: Göttingen, Germany, 1996.
(17) Sheldrick, G. M. *SHELXS 97, Program for crystal structure refinement*; University of Göttingen: Göttingen, Germany, 1997.
(18) For most hydrogen bonds between O atoms, the O···O separations fall in the range of 2.50−2.80 Å: Pauling, L. *The Nature of the Chemical Bond*, 3rd ed.; Cornell University Press: Ithaca, New York, 1960; pp 484−485.

Table 2. Selected Mean Interatomic Distances (Å) and Angles (deg) in Face-Centered Cubic Clusters of the Type $[Tp_8(H_2O)_xM_6Fe_8(CN)_{24}]$ (M = Co, Ni, Cu)

	Co_6Fe_8 (**1**)	Ni_6Fe_8 (**2**)	Cu_6Fe_8[a]
Fe−C	1.891(6)	1.91(2)	1.909(4)
Fe−N	1.925(8)	1.93(2)	1.824(2)
M−N	2.023(5)	2.03(2)	1.967(3)
M−O	2.079(2)	2.24(3)	2.155(5)
C≡N	1.17(1)	1.13(5)	1.148(6)
Fe···Fe	6.948(2)	6.97(1)	6.88(1)
Fe···M	5.066(1)	5.02(1)	4.94(1)
M···M	6.662(3)	6.28(1)	6.36(1)
	9.421(5)	8.88(1)	8.90(1)
Fe−C−N	179.5(9)	180(4)	174.2(3)
M−N−C	171.8(9)	164(4)	173.8(3)
C−Fe−C	87.5(2)	86(1)	87.5(3)
C−Fe−N	92.6(1)	93.7(4)	85.4(4)
N−Fe−N	87.2(2)	85.9(9)	98.4(1)
N−M−N	88.61(5)	89.95(4)	88.4(2)
	162.1(3)	177(1)	165.4(2)
N−M−O	88.9(1)	90.0(4)	99.6(1)

[a] Ref 14.

Magnetic susceptibility data were collected in the 2−300 K temperature range using a Quantum Design MPMS XL-7 SQUID magnetometer. To prevent desolvation of the samples, the measurements were performed on crystals frozen in THF and sealed in a borosilicate tube under vacuum. All data were corrected for diamagnetic contributions employing both a background subtraction of the sample holder with solvent and Pascal's constants. Magnetization data were fit with the Hamiltonian $\hat{H} = D\hat{S}_z^2 + E(\hat{S}_x^2 + \hat{S}_z^2) + g\mu_B\mathbf{SB}$ using ANISOFIT 2.0, where the μ_B is the Bohr magneton and *g*, *D*, *E*, **S**, and **B** represent the Landé *g* factor, the axial and rhombic zero-field splitting parameters, and the spin and magnetic field vectors, respectively.[13]

Results and Discussion

Syntheses. The synthetic approach employed paralleled that previously reported for the preparation of $[Tp_8(H_2O)_6Cu_6Fe_8(CN)_{24}](ClO_4)_4\cdot 12H_2O\cdot 2Et_2O$.[14] Self-assembly reactions involving $M(ClO_4)_2\cdot 6H_2O$ (M = Co, Ni) and $K[TpFe(CN)_3]$ in a 1:1 mixture of methanol and acetonitrile proceeded as follows:

$$6M(ClO_4)_2\cdot 6H_2O + 8K[TpFe(CN)_3] \rightarrow [Tp_8(H_2O)_{12}M_6Fe_8(CN)_{24}](ClO_4)_4 + 8KClO_4 + 24H_2O \quad (3)$$

We speculate that the precipitation of the colorless solid $KClO_4$ may provide the driving force for cluster formation. Separation of the precipitate by filtration, followed by diffusion of THF vapor into the filtrate, affords solvates of the cluster-containing compounds $[Tp_8(H_2O)_{12}Co_6Fe_8(CN)_{24}](ClO_4)_4\cdot 12THF\cdot 7H_2O$ (**1**) and $[Tp_8(H_2O)_{12}Ni_6Fe_8(CN)_{24}](ClO_4)_4\cdot 12THF\cdot 7H_2O$ (**2**) in pure form. It is important to note that dry solvents are required because the reaction does not proceed in the presence of excess water. Analogous reactions carried out with $Mn(ClO_4)_2\cdot 6H_2O$ or $Fe(ClO_4)_2\cdot 6H_2O$ appeared to give similar results, but the poor quality of the ensuing crystals has thus far precluded structure determination.

Crystal Structures. Compounds **1** and **2** are isostructural, both crystallizing in space group $Pm\bar{3}m$. Selected mean interatomic distances and angles are listed in Table 2. As

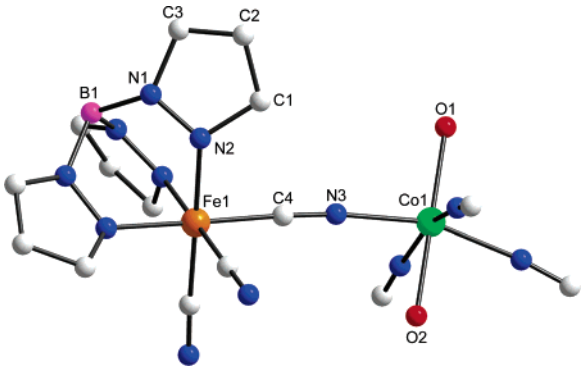

Figure 1. Structure of a fragment of the face-centered cubic cluster in **1** showing the asymmetric unit (labeled atoms) and the coordination geometry at each metal site. Hydrogen atoms are omitted for clarity.

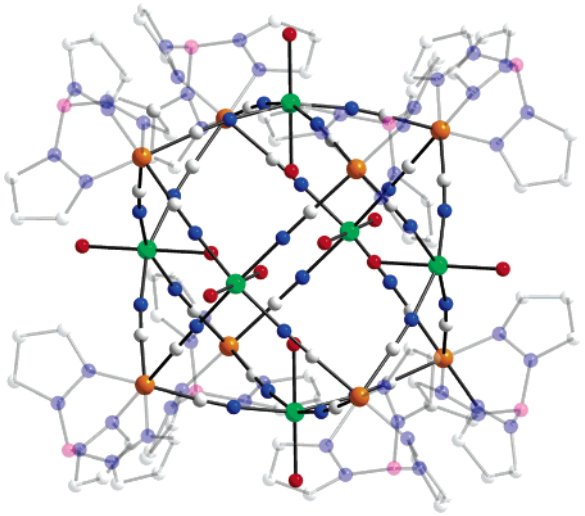

Figure 2. Structure of the face-centered cubic $[Tp_8(H_2O)_{12}Co_6Fe_8(CN)_{24}]^{4+}$ cluster in **1**. Orange, green, purple, gray, blue, and red spheres represent Fe, Co, B, C, N, and O atoms, respectively; H atoms have been omitted for claity. The Tp^- ligands are drawn transparently for better visualization of the core structure. The molecule resides on an O_h symmetry site within the crystal. The $[Tp_8(H_2O)_{12}Ni_6Fe_8(CN)_{24}]^{4+}$ cluster in **2** is isostructural.

shown in Figure 1, each Fe^{III} center retains the octahedral coordination environment of the $[TpFe(CN)_3]^-$ precursor complex, while each Co^{II} or Ni^{II} center displays an octahedral coordination sphere composed of four N-bound cyanide ligands and two trans water ligands. The Fe−C distances of 1.891(6) and 1.91(2) Å are shorter than the M−N distances of 2.023(5) and 2.03(2) Å, consistent with the anticipated Fe−C≡N−M linkages. The cyanide bridges are nearly linear in **1**, with Fe−C−N and Co−N−C angles of 179.5(9) and 171.8(9)°, respectively, but are quite bent at the N end in **2**, with Fe−C−N and Ni−N−C angles of 180(4) and 164(4)°, respectively. The two Co−O distances of 2.10(1) and 2.078(2) Å in **1** are comparable and slightly shorter than the two Ni−O distances of 2.23(4) and 2.24(2) Å in **2**.

The structure of the $[Tp_8(H_2O)_{12}Co_6Fe_8(CN)_{24}]^{4+}$ cluster in **1** is depicted in Figure 2. It consists of a cube of eight Tp^--capped Fe^{III} centers connected via bridging cyanide ligands to six Co^{II} centers, one located just above the center of each cube face. This metal−cyanide framework is analogous in connectivity to the frameworks observed in two previously reported face-centered cubic clusters: $[(tach)_8(H_2O)_6Cu_6Co_8(CN)_{24}\supset THF]^{12+}$ (tach = 1,3,5-triaminocyclohexane)[6a] and $[Tp_8(H_2O)_6Cu_6Fe_8(CN)_{24}]^{4+}$.[14] Significantly, however, these species exhibit square pyramidal coordination at the face-centering Cu^{II} sites, whereas **1** and **2** demonstrate for the first time that such sites can be occupied by octahedrally coordinated metal centers. Here, the six coordinated water molecules are directed toward the cavity with O···O separations of 3.723 Å in **1** and 3.23 Å in **2**. This considerable difference is associated with the larger *trans*-M···M separation of 9.421(5) Å in **1** versus 8.88(1) Å in **2**, as well as the less bent M−N−C angle in **1**. A related difference is evident in the comparison of the distances between the Fe_4 plane of a cube face and the M centers: 1.237(7) Å in **1** and 0.959(8) Å in **2**. Comparisons with the structure of $[Tp_8(H_2O)_6Cu_6Fe_8(CN)_{24}]^{4+}$ (see Table 2) show this species to be closer in *trans*-M···M separation to the Co_6Fe_8 cluster but more similar in cyanide bridge angles to the Ni_6Fe_8 cluster.

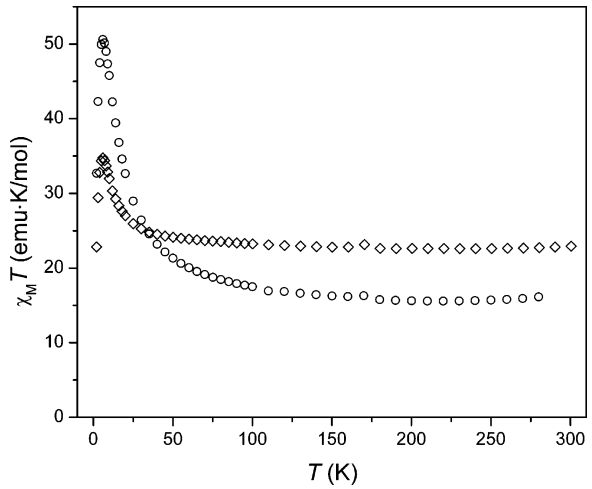

Figure 3. Temperature dependence of $\chi_M T$ for **1** (diamonds) and **2** (circles) measured at 5000 Oe.

Importantly, the octahedral coordination geometry at the Ni^{II} centers in **2** can be expected to preserve a high-spin ($S = 1$) electron configuration. In contrast, the cyanide linkage isomerization observed in the formation of face-centered cubic clusters such as $[(Me_3tacn)_8Cr_8Ni_6(CN)_{24}]^{12+}$ results in a square planar coordination and a low-spin ($S = 0$) electron configuration at the face-centering Ni^{II} sites.[12] Thus, the $[Tp_8(H_2O)_{12}Ni_6Fe_8(CN)_{24}]^{4+}$ cluster provides a structural model for the high-spin green intermediate "$[(Me_3tacn)_8(H_2O)_{12}Ni_6Cr_8(CN)_{24}]^{12+}$" species (with a putative $S = 18$ ground state) that precedes cyanide ligand reorientation.[12]

The face-centered cubic clusters are well isolated within the crystal structures. The closest metal−metal contacts between neighboring clusters are Co···Co distances of 8.124(3) Å in **1** and Ni···Ni distances of 8.66(1) Å in **2**. In addition, no short hydrogen-bonding pathways are apparent between clusters. Thus, it can be anticipated that the magnetic properties observed for the compounds will be primarily those of the individual cluster molecules.

Magnetic Properties. The dc magnetic susceptibility data were measured for **1** and **2** in the temperature range of 2−300 K (see Figure 3). At room temperature, the observed $\chi_M T$ values are 22.9 emu K mol^{-1} for **1** and 16.1 emu K mol^{-1}

for **2**. The former is within the normal range of 19.0−26.4 emu K mol^{-1} for eight low-spin Fe^{III} centers and six high-spin Co^{II} centers in the absence of exchange coupling, while the latter is slightly above the normal range of 10.3−13.8 emu K mol^{-1} for eight low-spin Fe^{III} centers and six high-spin Ni^{II} centers.[19] The $\chi_M T$ values for both compounds remain nearly invariant down to ∼100 K, and then they increase to maxima of 34.7 emu K mol^{-1} at 6 K for **1** and 50.6 emu K mol^{-1} at 6 K for **2**, before abruptly decreasing at lower temperatures. This behavior is indicative of ferromagnetic exchange coupling, which is further supported by the positive Weiss constants ($\Theta = 2.8$ K for **1** and 8.0 K for **2**) extracted from linear fits to plots of $1/\chi_M$ versus T. Clearly, the strength of the exchange coupling is greater within the Ni_6Fe_8 cluster of **2** than in the Co_6Fe_8 cluster of **1**. The downturn in the $\chi_M T$ values observed at very low temperature in each case likely stems from a combination of zero-field splitting and the Zeeman effects associated with a high-spin ground state.

The observation of ferromagnetic exchange coupling between Fe^{III} and Co^{II} in **1** is surprising in view of the antiferromagnetic coupling recently reported for the cyano-bridged clusters $[Tp^*_2(DMF)_8Co_2Fe_2(CN)_6]^{2+}$ (Tp^* = hydridotris(3,5-dimethylpyrazol-1-yl)borate)[20] and $[Tp_4(MeCN)_2(H_2O)_4Co_2Fe_4(CN)_{12}]$.[21] The Co^{II} centers in these clusters each display two or three $Co^{II}-NC-Fe^{III}$ connections arranged in cis and mer orientations, respectively, while in $[Tp_8(H_2O)_{12}Co_6Fe_8(CN)_{24}]^{4+}$, the Co^{II} centers exhibit four such connections arranged in an equatorial plane. When the electron configuration of $t_{2g}^5e_g^2$ for high-spin Co^{II} in a pseudooctahedral ligand field is taken into account, the two unpaired electrons occupying the e_g orbitals would be expected to give rise to ferromagnetic contributions to the exchange coupling with the single unpaired electron of the low-spin Fe^{III} centers (t_{2g}^5) because of the predominate orthogonality, while the one unpaired electron in the t_{2g} orbitals of Co^{II} would impart a competing antiferromagnetic contribution.[22] The nature of the exchange coupling in clusters built up of $Fe^{III}-CN-Co^{II}$ linkages may therefore be quite sensitive to the number and arrangement of the cyanide bridges around the Co^{II} center, as well as to the ligand field properties of its terminal ligands. This hypothesis is consistent with the observation that the exchange coupling in $[Tp_4(MeCN)_2(H_2O)_4Co_2Fe_4(CN)_{12}]$ switches from antiferromagnetic to ferromagnetic upon desolvation of the sample, which presumably forges additional $Fe^{III}-CN-Co^{II}$ linkages.[21] Indeed, it may even be possible to switch the coupling in $[Tp_8(H_2O)_{12}Co_6Fe_8(CN)_{24}]^{4+}$ from ferromagnetic to antiferromagnetic, simply by replacing its water ligands with ligands of a different field strength. Note that ferromagnetic coupling has also been observed between Fe^{III} and Co^{II} centers in the trigonal bipyramidal cluster $[Tp_3(Tpm^{Me})_2Fe_3Co_2(CN)_9]^+$ (Tpm^{Me} = tris(3,5-dimethyl-1-pyrazoyl)methane)[23] and in two separate chain compounds, one of which features the same $Co(CN)_4(H_2O)_2$ coordination environment as seen in **1**.[24,25]

The situation for compound **2** is more straightforward. Here, the strict orthogonality between the spin orbitals of Fe^{III} (t_{2g}^5) and Ni^{II} ($t_{2g}^6e_g^2$) leads to the observed ferromagnetic exchange coupling,[22] and analogous behavior has been reported for a variety of other iron(III)−nickel(II)−cyanide clusters.[5,26]

To further probe the ground state magnetic properties of the clusters in **1** and **2**, field-dependent magnetization data were collected in the temperature range of 2−8 K (see Figure 4). For compound **1**, the magnetization values at the highest field applied exhibit saturation at 22.0 μ_B, somewhat lower than the expected 26 μ_B expected for an $S = 13$ ground state with $g = 2.00$. This can be attributed to the presence of a significant zero-field splitting, as also indicated by the large separations between isofield lines. Note also that the values are higher than could be reasonably accounted for with a spin ground state of $S = 5$, as would be expected in the case of antiferromagnetic exchange coupling. Attempts to fit the data with an $S = 13$ ground-state spin, assuming $S = {}^3/_2$ for Co^{II}, gave an exceptionally large zero-field splitting parameter of $D = 27.7$ cm^{-1}, together with $E = 0.34$ cm^{-1} and $g = 2.563$. In some cases, however, Co^{II} centers have been treated as having an effective spin of $S' = {}^1/_2$ in the low-temperature range, associated with the Kramers doublets generated from the combined effects of spin−orbit coupling and a distorted octahedral geometry.[27] Fits to the low-temperature magnetization data assuming a ground state $S = 7$ stemming from ferromagnetic coupling and the effective spin $S' = {}^1/_2$ for Co^{II} indeed gave more reasonable fit parameters with $D = -0.544$ cm^{-1}, $E = 0.0331$ cm^{-1}, and $g = 2.996$ (Figure 4). These values are quite close to those reported for $[Tp_3(Tpm^{Me})_2Fe_3Co_2(CN)_9]^+$ [23] and are more reasonable in view of the high symmetry of the face-centered cubic cluster.

For compound **2**, the magnetization data for the highest-applied field saturate at 23.9 μ_B, which is slightly above the value of 20 μ_B expected for an $S = 10$ ground state with $g = 2.00$. This result suggests a g value of greater than 2.00, while the separations in the isofield lines again indicate the presence of zero-field splitting. Attempts to model the data

(19) Casey, A. T.; Mitra, S. In *Theory and Applications of Molecular Paramagnetism*; Boudreaux, E. A., Mulay, L. N., Eds.; John Wiley & Sons: New York, 1976. The reported range of $\chi_M T$ values for octahedral complexes is 0.56−0.75 emu K mol^{-1} for low-spin Fe^{III} (p 190), 2.42−3.40 emu K mol^{-1} for high-spin Co^{II} (p 214), and 0.97−1.30 emu K mol^{-1} for Ni^{II} (p 226).
(20) Li, D.; Parkin, S.; Wang, G.; Yee, G. T.; Prosvirin, A. V.; Holmes, S. M. *Inorg. Chem.* **2005**, *44*, 4903.
(21) Kim, J.; Han, S.; Pokhodnya, K. I.; Migliori, J. M.; Miller, J. S. *Inorg. Chem.* **2005**, *44*, 6983.
(22) Weihe, H.; Güdel, H.-U. *Comments Inorg. Chem.* **2000**, *22*, 75.
(23) Gu, Z.-G.; Yang, Q.-F.; Liu, W.; Song, Y.; Li, Y.-Z.; Zuo, J.-L.; You, X.-Z. *Inorg. Chem.* **2006**, *45*, 8895.
(24) Lescouëzec, R.; Vaissermann, J.; Ruiz-Pérez, C.; Lloret, F.; Carrasco, R.; Julve, M.; Verdaguer, M.; Dromzee, Y.; Gattechi, D.; Wernsdorfer, W. *Angew. Chem., Int. Ed.* **2003**, *42*, 1483.
(25) Toma, L. M.; Lescouëzec, R.; Lloret, F.; Julve, M.; Vaissermann, J.; Verdaguer, M. *Chem. Commun.* **2003**, 1850.
(26) Li, D. F.; Clerac, R.; Parkin, S.; Wang, G. B.; Yee, G. T.; Holmes, S. M. *Inorg. Chem.* **2006**, *45*, 5251.
(27) (a) Plater, M. J.; Foreman, M. R. J.; Coronado, E.; Gómez-García, C. J.; Slawin, A. M. Z. *J. Chem. Soc., Dalton Trans.* **1999**, 4209. (b) Brechin, E. K.; Cador, O.; Caneschi, A.; Cadiou, C.; Harris, S. G.; Parsons, S.; Vonci, M.; Winpenny, R. E. P. *Chem. Commun.* **2002**, 1860.

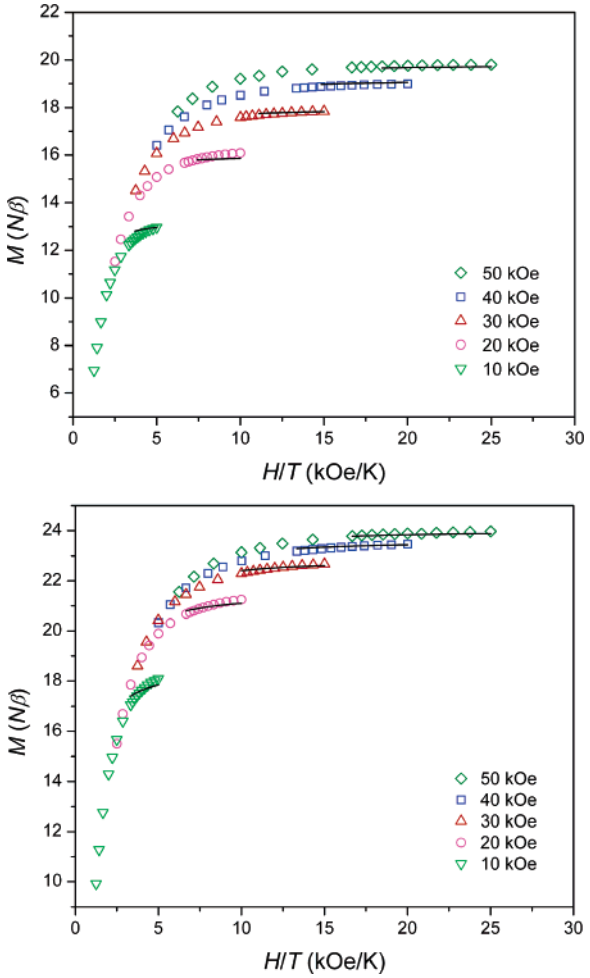

Figure 4. Low-temperature magnetization data for **1** (top) and **2** (bottom) measured at various applied magnetic fields. Solid lines represent fits to the data, as calculated using ANISOFIT 2.0.

using ANISOFIT 2.0 gave a best fit with the parameters $g = 2.475$, $D = 0.21$ cm^{-1}, and $E = 0.064$ cm^{-1} for the $S = 10$ ground state.

Although powder magnetization measurements are not necessarily reliable in establishing the sign of D, the best fits in each case indicate that the axial zero-field splitting should be of sizable magnitude; ac magnetic susceptibility measurements were therefore performed at various switching frequencies to check for slow relaxation effects (see Figure S1 in the Supporting Information). For both compounds, the absence of an out-of-phase magnetic susceptibility signal confirms the lack of single-molecule magnet behavior.

Outlook

These results demonstrate that octahedral metal centers can in fact be incorporated at the face-centering sites of face-centered cubic clusters, opening up access to many more high-spin ground states for the geometry. Although the new clusters $[Tp_8(H_2O)_{12}M_6Fe_8(CN)_{24}]^{4+}$ (M = Co, Ni) possess higher-spin ground states and increased zero-field splitting relative to $[Tp_8(H_2O)_6Cu_6Fe_8(CN)_{24}]^{4+}$, they unfortunately do not exhibit single-molecule magnet behavior because of their positive D values. Nevertheless, it is possible that other combinations of metal centers within this geometry will retain a negative D parameter. In addition, the possibility of performing ligand substitutions at the outer terminal water ligand sites may enable incorporation of the clusters into larger molecular assemblies or even extended coordination solids. Future work will focus on these ideas, as well as on breaking the cubic symmetry of the clusters via substitution of a heterometal ion onto a corner or face-centering metal site.[28]

Acknowledgment. This work was supported by the National Science Funds for Distinguished Young Scholars of China (20625103), the Natural Science Foundations of China (Grant 20371051) and Guangdong Province (Grant 04205405), as well as the U.S. National Science Foundation (Grant CHE-0617063).

Supporting Information Available: Ac magnetic susceptibility data for **1** and **2** (PDF) and X-ray crystallographic files (CIF). This material is available free of charge via the Internet at http://pubs.acs.org.

IC061924B

(28) Freedman, D. E.; Bennett, M. V.; Long, J. R. *Dalton Trans.* **2006**, 2829−2834.